

Estimation of the Myocardium Rotation from Standard Cine Magnetic Resonance Imaging Sequences

Amro Ahmed¹, Mohamed Abouelhoda^{1,2}, Ayman Khalifa³, Ahmed S. Fahmy^{1,2}

¹Center for Informatics Science (CIS), Nile University (NU)

²Systems and Biomedical Engineering Department, Cairo University

³Systems and Biomedical Engineering Department, Helwan University
Cairo, Egypt

ABSTRACT

Myocardium rotation and torsion are important indicators of the cardiac function. Currently, *tagged* Magnetic Resonance Imaging (tMRI) sequences are analyzed to estimate these parameters. Unfortunately, tMRI is not widely used in clinical practice because it prolongs the scanning time and requires sophisticated analysis software. In this work, we present a method for estimating the myocardium rotation from *standard* cine MRI sequences. The method is based on identifying special features, i.e. landmarks, of the intensity pattern around the myocardium borders at each timeframe. Each set of landmarks is then encoded using a string of characters that can be matched across the different timeframes. String alignment technique is used to match the characters and thus determine the inter-frame motion of each landmark. Preliminary results using dataset of three patients (apical, mid, and basal slices) indicate the potential of the method to estimate the myocardium rotation especially at late timeframes where tMRI fails due to tag fading.

Index Terms— Myocardium, rotation, MRI, string alignment

1. INTRODUCTION

Steady State Free Precision (SSFP) imaging technique is a standard image acquisition protocol in Magnetic Resonance Imaging (MRI) [1]. The technique provides high quality cine sequences of the heart that can be used to assess many cardiac functional parameters. This includes ejection fraction; systolic, diastolic and stroke volumes; ventricular volume and mass; and wall thickness and thickening [2]. Other functional parameters such as myocardium rotation and torsion are important indicators of myocardium infarction [3]. Nevertheless, estimation of these parameters from SSFP sequences using conventional tracking methods, such as optical flow, is usually hindered by many obstacles. For example, the lack of significant tissue texture in SSFP images limits the sensitivity of the tracking algorithm. In addition, the rapid myocardium motion combined

with low temporal resolution of the imaging sequence can lead to failure of the tracking algorithm [4].

Currently, tagged MRI (tMRI) imaging sequences are considered the golden reference for estimating the myocardium rotation and torsion [5]. Nevertheless, tMRI is not common in the practice of cardiac imaging due to some technical limitations. First, acquisition of tMRI sequences significantly increases the time, and hence the cost, of the patient scans. Secondly, fading of the image tags limits the accuracy and the reliability of most analysis techniques especially at late cardiac phases.

In this work, we present method for estimating the myocardium rotation from standard SSFP image sequences. The method is based on identifying special features, i.e. landmarks, of the intensity pattern around the myocardium borders at each timeframe. Each set of landmarks is then encoded using a string of characters that can be matched across the different timeframes. String alignment technique is used to match the characters and thus determine the inter-frame motion of each landmark [6].

2. THEORY & METHODS

Five main steps are required to estimate the myocardium rotation. The input of the proposed method is a segmented sequence of cardiac SSFP images. As will be shown below, the segmentation is not crucial to the performance of the proposed methods because only rough delineation of the myocardium borders is needed. In this work, active contour (ACM) based segmentation method is used to extract the myocardium contours at each timeframe [6].

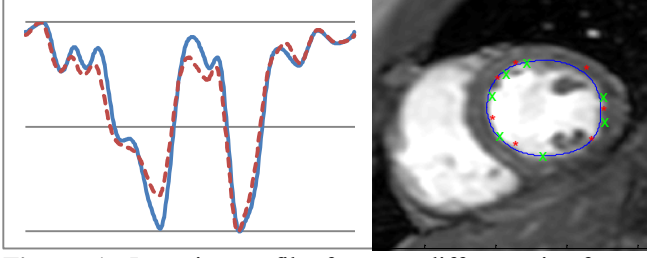


Figure 1. Intensity profile for two different timeframes (left). The peaks and valleys of the blue profile are indicated by the red and green 'x' on the myocardium contour (right).

2.1 Intensity Profiles of the Myocardium Contours

At timeframe, t , let C^t be a myocardium contour that comprises a set of N points: $\{P_n^t, n = 1:N\}$. Centered at each contour point, a line segment of length, L , is drawn perpendicular to the contour and the summation of the image intensity along this line is calculated. This results in a signal of length N that represents the intensity profile along the myocardium contour. Usually, N is set to 360 and L is set to 10 pixels. The resulting profile is then normalized to vary from 0 to 1. It is worth noting that because the summation is taken over a relatively long line, the exact location of the segmented contour points, does not significantly impact the resulting intensity profiles. Figure 1 shows the intensity profile for two consecutive timeframes. The y- and x-axes are the normalized intensity and the angle in degrees of each contour point.

2.2. Identifying Contour Landmarks

In order to estimate the rotational motion of the myocardium, some landmarks on the intensity profile (obtained from the previous step) have to be identified. In this work, the local maxima and minima are taken as the desired landmarks. In order to avoid noise effect, a low pass averaging filter (of size 1x5) is applied to the intensity profile prior to determining the landmarks. Then, the profile is searched for a change in the slope to locate the local maxima and minima. This results in a number of landmarks, K^t , that is variable from one timeframe to another. The image on the right in Fig. 1 shows the contour and the location of the peaks and valleys landmarks detected by the algorithm.

2.3. Encoding of the Landmarks

To capture the intrinsic properties of each landmark, we propose a scheme that encodes the magnitude and width of each landmark into a string over a finite alphabet. First, the normalized magnitude (ranging from 0 to 1) is quantized into 5 levels, as shown in Figure 2. For profile landmarks representing

local maxima, we map these levels to five characters, denoted by a, b, c, d , and e . For profile landmarks representing local minima, we map the same levels to a different set of characters, denoted by s, t, u, v , and w . Secondly, the non-landmark locations on the intensity profiles are given the label: l . That is, we have an alphabet Σ of 11 characters to which the levels are mapped. For example, Figure 2 shows a part of a landmark profile including two maxima and one minimum with magnitudes 0.9, 0.7, and 0.1, respectively. The spacing between the first peak and the minimum is 5 units, while the distance between the minimum and the second maximum is 3 units. The string S that encodes this profile is $ELLLLLSLLLD$.

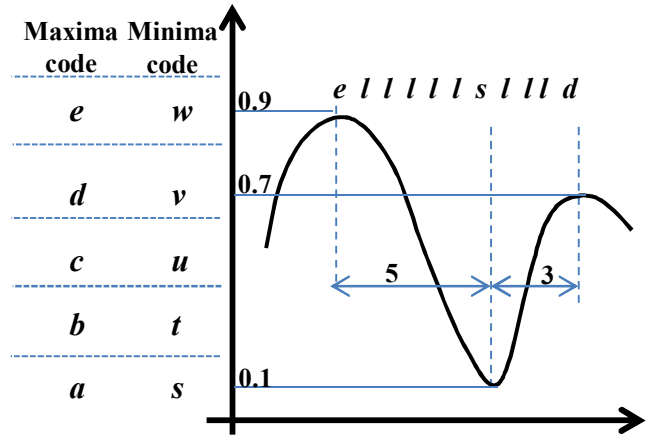


Figure 2. Example of an Intensity profile encoding.

For string alignment purpose, we define a distance measure between the different characters in Σ . For two characters s and s' , we define the distance $d(s, s')$ as the difference between their corresponding numerical values. For example, the distance between the pairs of characters (a, b) , (a, e) , (a, l) , and (s, v) are equal to 1, 4, 11, 18, and 3 respectively.

2.4. String Alignment

String alignment is a method for comparing two strings to identify regions of similarity and differences. Let $S[1..n]$ and $R[1..m]$ denote two string S and R of lengths n and m , respectively. In our model S and R represent two myocardium contours (C^t and C^{t+1}) at two different time frames t and $t+1$. We define three operations working on characters of the strings: 1) *Match*, where character a matches b in the alignment; 2) *Insertion*, where a character a is inserted in S or R ; and 3) *Deletion*, where a character a is deleted from S or R . Each of these operations has a numerical cost defined as follows: The cost of matching a to b is the distance $d(a, b)$. The insertion and deletion cost is set to a fixed value δ . The optimal global alignment is to arrange the characters of S and R from left to right

using this set of operations such that the total cost of all operations is minimal. (It is also equivalent to say that we optimally transform S into R using this set of operations). Figure 3 shows an example of two strings and an optimal alignment of them.

S:	E L L L L S L L L D	R:	E L L L S L C L D
Alignment of	E L L L L S L - L L D		
S and R	E L L L - S L C L - D		

Figure 3. Alignment of two strings S and R : The matched characters are placed above each other. The ‘-’ symbol refers to insertion/deletion.

The minimum alignment cost can be computed using the dynamic programming scheme [8]. Let $A[i, j]$ denote the minimum cost of aligning the prefix $S[1..i]$ to the prefix $R[1..j]$, we use the following recurrence to compute $A[i, j]$.

$$A[i, j] = \min \begin{cases} A[i-1, j-1] + d(S[i], R[j]) \\ A[i-1, j] + \delta \\ A[i, j-1] + \delta \end{cases}$$

and $A[0, j] = j \times \delta$ and $A[i, 0] = i \times \delta$. Putting $i=n$ and $j=m$, $A[n, m]$ is the score of an optimal alignment of S and R . This recurrence can be easily computed by establishing a matrix A and filling it either row- or column-wise. This yields an algorithm with $O(nm)$ time and space. To report an optimal alignment as in Figure 3, a trace-back procedure is applied to recover the involved operations [8].

2.5. Estimation of the Myocardium Rotation

The string alignment step yields a map that links a number of landmarks, M , in one contour, P_m^t , to the matching points in the other contour, P_m^{t+1} , where $m=1:M$. Assuming a rigid body motion, the rotation angle, θ , of the myocardium between the two timeframes can be estimated by simultaneously solving the following system of equations for all values of m ,

$$\begin{aligned} x_m^t \cos(\theta) + y_m^t \sin(\theta) &= x_m^{t+1} \\ x_m^t \sin(\theta) - y_m^t \cos(\theta) &= y_m^{t+1} \end{aligned}$$

The solution of the above equation yields two values: $\cos(\theta)$ and $\sin(\theta)$. The latter is used to estimate θ because the sine function is linear and thus more sensitive at the small values of the myocardium rotation (typically few degrees).

2.6. Test and Validation

The dataset used for testing and validation is composed of tMRI and SSFP image sequences for five patients. Both sequences capture the same cross sections of each patient (apical, mid cavity, and basal slices). The tMRI sequences contain 13-15 timeframe while the SSFP sequences contain 20-25 timeframe. The tMRI images are analyzed to estimate the myocardium rotation at each timeframe using the HARP tracking technique [7]. The SSFP images are analyzed using the proposed methods. For comparison purpose, the rotation angles from the SSFP are interpolated and truncated to calculate the rotation angles at exactly the same timeframe point given by the tMRI sequence. The correlation between the resulting angles of both techniques for each patient (for the apical, mid, and basal slices) is calculated to test the accuracy of the proposed methods.

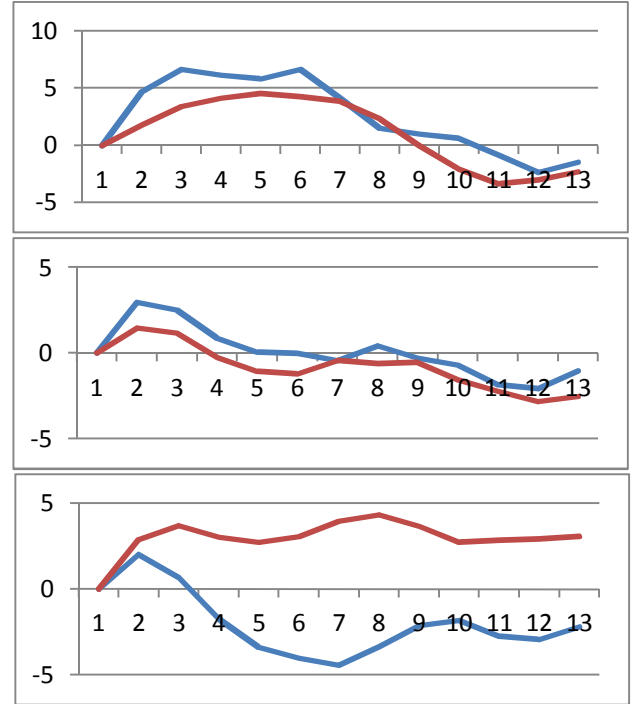


Figure 4. Myocardium rotational angle vs. timeframes estimated by the proposed method (blue) and HARP (red) for apical, mid-cavity, and basal slices of one patient. ($r=0.92, 0.93, 0.36$).

3. RESULTS AND DISCUSSION

Considering the angular rotation between the consecutive timeframes, the correlation coefficient, r , between the values estimated by the HARP and the proposed technique was found as listed in Table 1. As can be shown in the table, the correlation is lowest in the basal slices. This can be due to the vigorous motion of the (loose) papillary muscles in the basal slices. Taken the first timeframe as a reference, the

overall rotation angle of the myocardium can be calculated by accumulating the individual rotation angles between the consecutive timeframes. Figure 4 shows the overall myocardium rotation for one patient at the apical, mid-cavity and basal slices. The red and blue curves respectively represent the angles estimated using the proposed method and the HARP technique. The correlation coefficient between each pair of curves in this figure is 0.92, 0.93 and 0.36. It is worth noting that, the low correlation in the basal slice is due to erroneous values at the beginning of the cardiac cycles that propagate through the timeframes.

Table 1. Myocardium rotation angle bet

	Apex	Mid	Base
Patient1	0.83	0.55	0.71
Patient2	0.81	0.46	0.48
Patient3	0.63	0.79	0.42

Figure 5 shows a scatter plot of the rotation angles estimated from the tagged MRI using HARP and from the cine SSFP using the proposed method. The overall correlation coefficient is 0.59 with p-value less than 0.01, which means significant correlation between the two techniques.

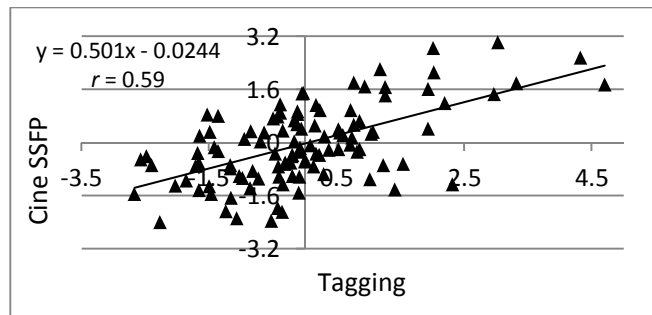


Figure 5. Scatter plot of the rotation angles estimated from tagged MRI and from the cine SSFP ($r=0.59$, $p\text{-value}<0.01$).

4. CONCLUSION

In this work, we have presented a method for estimating myocardium rotation from standard SSFP MRI sequences. The new method is fast and does not require sophisticated processing with the preliminary results confirm its potential to estimate the torsion. The significance of this method is to allow the estimation of functional parameters that currently cannot be estimated from standard SSFP sequences.

ACKNOWLEDGMENTS

This work is supported by a grant from the Science and Technology Development Fund (STDF #1979), Cairo, Egypt.

REFERENCES

- [1] H. Thiele, E. Nagel, I. Paetsch, et al., "Functional cardiac MR imaging with steady-state free precession (SSFP) significantly improves endocardial border delineation without contrast agents," *J Magn Reson Imaging*, vol 14, pp 362–7, 2001.
- [2] V. B. Ho, T. K. F. Foo, "Impact of Cine MR Imaging: Potential for the Evaluation of Cardiovascular Function," *American Journal of Radiology (AJR)*, vol. 187, pp. 605-8, 2006.
- [3] T. Arts, S. Meerbaum, and R. S. Reneman, "Torsion of the left ventricle during the ejection phase in the intact dog," *Cardiovasc. Res.*, vol. 18, pp.183, 1984.
- [4] S. C. Amartur and H. J. Vesselle, "A new approach to study cardiac motion: The optical flow of cine MR images," *Magnetic Resonance in Medicine*, vol. 29, pp. 59–67, 1993.
- [5] M.J.W. Götte, et al.: "Myocardial Strain and Torsion Quantified by Cardiovascular Magnetic Resonance Tissue Tagging," *J. Am. Coll. of Cardiol.* 48, pp 2002-11, 2006.
- [6] Ahmed S. Fahmy, Ahmed ElAgamy, Ayman Khalifa, "Myocardial Segmentation Using Contour Constrained Optical Flow Tracking," *Proc. of STACOM workshop, MICCAI 2012, LNCS*, vol. 7085, pp 120-8, 2012.
- [7] N. F. Osman, W. S. Kerwin, E. R. McVeigh, J. L. Prince, "Cardiac Motion Tracking Using CINE Harmonic Phase (HARP) Magnetic Resonance Imaging," *Magn Reson Med*, vol. 42, pp1048-60, 1999.
- [8] D. Gusfield, *Algorithms on strings, trees, and sequences: computer science and computational biology*. Cambridge, UK: Cambridge University Press. pp. 263–264, 1997.